HAL
archives-ouvertes.fr

RNA interference is essential for cellular quiescence

B. Roche, Benoît Arcangioli, R. Martienssen

▶ To cite this version:

B. Roche, Benoît Arcangioli, R. Martienssen. RNA interference is essential for cellular quiescence. Science, American Association for the Advancement of Science, 2016, 354 (6313), 10.1126/science.aah5651 . pasteur-01868276

HAL Id: pasteur-01868276
https://hal-pasteur.archives-ouvertes.fr/pasteur-01868276

Submitted on 13 Feb 2019

HAL is a multi-disciplinary open access archive for the deposit and dissemination of scientific research documents, whether they are published or not. The documents may come from teaching and research institutions in France or abroad, or from public or private research centers.

L'archive ouverte pluridisciplinaire **HAL**, est destinée au dépôt et à la diffusion de documents scientifiques de niveau recherche, publiés ou non, émanant des établissements d'enseignement et de recherche français ou étrangers, des laboratoires publics ou privés.

Distributed under a Creative Commons Attribution| 4.0 International License

Title:

RNA interference is essential for cellular quiescence.

Authors:

Roche, B.[1], Arcangioli, B.[2] and Martienssen, R.A.[1] *

Affiliations:

1. Howard Hughes Medical Institute—Gordon and Betty Moore Foundation, Cold Spring Harbor Laboratory, 1 Bungtown Road, Cold Spring Harbor NY11724, USA.

2. Institut Pasteur, Dynamic of the Genome Unit, Department of Genomes and Genetics, UMR3525, 25-28 rue du Docteur Roux, Paris 75015, France.

* Correspondence to: martiens@cshl.edu

Abstract:

Quiescent cells play a predominant role in most organisms. Here, we identify RNA interference (RNAi) as a major requirement for quiescence (G_0) in *Schizosaccharomyces pombe*. RNAi mutants lose viability at G_0-entry and are unable to maintain long-term quiescence. We obtained *dcr1*Δ G_0 suppressors, which mapped to genes involved in chromosome segregation, RNA polymerase-associated factors, and heterochromatin formation. We propose a model in which RNAi promotes RNA polymerase release in cycling and quiescent cells: (i) RNA pol II release mediates heterochromatin formation at centromeres allowing proper chromosome segregation during mitotic growth and G_0-entry, and (ii) RNA pol I release prevents heterochromatin formation at rDNA during quiescence maintenance. Our model may account for the co-dependency of RNAi and H3K9 methylation throughout eukaryotic evolution.

Main Text:

In nature, most cells exist in a non-dividing state (the 'G_0' phase of the cell cycle). This state is commonly referred to as 'quiescent' when cells are still metabolically active and able to re-enter the cell cycle given the appropriate signal. Examples of quiescent cells include stem cell niches *(1)*, neuronal progenitor cells *(2)* and memory T cells *(3)*. Yeasts and other micro-organisms are also able to enter a reversible quiescent state in response to environmental cues *(4)*, and in several pathogenic species this state allows persistence of infection in the host *(5)*. Despite their tremendous importance, the molecular pathways involved in quiescence entry, maintenance, and exit, are not well understood. Given that long-term stability and reversibility are hallmarks of quiescence, epigenetic mechanisms are likely involved, and we are studying their contribution to quiescence, using the fission yeast *Schizosaccharomyces pombe* as a model.

In *S. pombe*, synchronized entry into the reversible quiescent state is induced upon nitrogen starvation in the absence of a mating partner. Under these conditions the rod-shaped cells divide twice without growth and differentiate into quiescent G_0 cells, which retain viability and the ability to re-enter the cell cycle for more than 1 month *(4)*. G_0 cells have a characteristic transcriptome *(5, 6)*, morphology and metabolic response *(4, 7, 8)*. RNAi-guided heterochromatic silencing is a major epigenetic pathway in *S. pombe*, which has one copy of each of the key enzymes involved: Dicer (Dcr1), Argonaute (Ago1) and RNA-dependent RNA polymerase (Rdp1). Transcription of pericentromeric repeats on both strands by RNA polymerase II is thought to generate partially double-stranded RNAs, which are cleaved by Dcr1 to small RNAs (21-23nt). Small RNAs bound to Ago1 are targeted to homologous transcripts, and lead to the recruitment of Rdp1 to generate more template dsRNA. Subsequent engagement of the CLRC/Rik1 silencing complex, which includes the histone H3 lysine 9 (H3K9) methyltransferase Clr4, and the H3K4 demethylase Lid2, silences heterochromatic transcripts and reporter genes. This process is tightly regulated during S-phase in order to ensure heterochromatin inheritance *(10, 11)*, and is coupled to the DNA replication fork, which promotes heterochromatin spreading *(12)*. RNAi mutants are viable but lose silencing of the pericentromeric repeats *(13)* resulting in chromosome segregation defects *(14)*.

We induced prototrophic wild-type, *dcr1*Δ, *ago1*Δ and *rdp1*Δ strains into G_0 by nitrogen starvation, and determined viability at different time-points up to 15 days *(15)*. While the wild-type strain retained 88.5% viability after 15 days of G_0, *dcr1*Δ viability was reduced to 53.3% at 24h and then gradually decreased to 7.9% at 15 days. *rdp1*Δ and *ago1*Δ cells had comparable, though less severe viability defects (Fig. 1A; Fig. S1; Fig. S2). We distinguished two different phases in the loss of viability of RNAi mutant strains: initial loss, which is characterized either by cells failing to enter G_0 or by cells unable to exit G_0, and subsequent gradual loss of viability over time, indicative of a defect in quiescence maintenance. In accordance with a major defect in G_0-entry, there was an increase in the number of cells retaining a 'rod-like' shape (Fig. 1BD), resulting in a lower number of cell divisions after nitrogen-starvation (Fig. 1C). Mis-segregated DNA at the first division was readily detected by DAPI staining. Furthermore, while wild-type G_0-exiting cells displayed a 'schmoo' morphology at the first S-phase *(4)*, this was only observed for viable RNAi mutant cells (that form colonies when micro-isolated on rich medium) and not for the majority of inviable cells, supporting the idea that initial loss of viability reflects an inability to properly enter the quiescent state. Over time, refraction-negative (dead) and mis-shaped cells constituted an increasing proportion of RNAi defective G_0 cells (Fig. 1B). Interestingly, the dead cells were morphologically heterogeneous, by comparison with, for example, *tdp1*Δ mutants in DNA repair *(16)*, indicating that the loss of viability may be a complex effect.

To assess whether the G_0 phenotype of RNAi mutants was due to the loss of pericentromeric heterochromatin, we assayed *swi6*^{HP1}Δ, *chp2*^{HP1}Δ, and *clr4*Δ for viability in G_0. We observed that *chp2*Δ had a wild-type G_0 phenotype, and that *swi6*Δ and *clr4*Δ strains were affected only during G_0-entry and subsequently viable (Fig. S3ABC). In parallel, we treated the wild-type strain with trichostatin A (TSA) for 24 hours before G_0-induction; this treatment results in loss of heterochromatin, but only results in a minor loss of viability in G_0 (Fig. S3DE). These results indicate that whereas the G_0-entry loss of viability was common to RNAi and heterochromatin mutants, the loss of viability in quiescence maintenance of RNAi mutants was not due to loss of pericentromeric heterochromatin. The two distinct phases of viability loss therefore rely on two different mechanisms.

To further explore the function of RNAi during quiescence maintenance, we established a suppressor screen based on the sharp decrease in viability of *dcr1*Δ in G_0, as follows: a population of *dcr1*Δ cells was induced into G_0 by nitrogen-starvation (EMM-N media) for 1-3 days, and was then put back into the cell cycle in rich medium (YES media) for ~4-7 generations. The population was then re-induced into G_0, and the process repeated, alternating between quiescence and growth for up to 20 cycles (Fig. 2A). Cells carrying a spontaneous suppressor mutation have a fitness advantage at every cycle, and are progressively enriched in the culture. We tested the protocol for proof-of-concept using a known suppressor *(15)*. We subsequently performed the suppressor screen on >50 independent populations, and we identified 13 *dcr1*Δ independent suppressors by whole genome sequencing *(17)* and validation in backcrosses *(15)* (Fig. S4; Fig. S5). The suppressors fell into three main classes (Fig. 2B):

(i) Mutants in chromosome segregation and kinetochore assembly: *ndc80*-R523L*, ndc80*-P431L*, ndc80*-R137N*, klp5-del.* The Ndc80 mutants affect each of the functional domains of the protein: R137 is in the globular domain, P431 in a Dis1-interaction site *(18)*, R523 is in the second long tail of unknown function. The *klp5-del* allele consists of a short deletion with a frameshift at codon 772, resulting in a different 772-814 C-terminus.
(ii) Mutants in the CLRC/Rik1 complex and HP1: *rik1*-K812**, raf2*-G37V*, swi6*-W293**, swi6*-T278K, *rik1*-T942K, *clr4*-R126*, *clr4*-Y451*.
(iii) Mutants in RNA polymerase-associated factors: *tbp1*-D156Y*, med31-ins*. The insertion in *med31-ins* consists of the replacement of Phe23 by the sequence LVRIC, without frameshift. This phenylalanine is highly conserved from budding yeast Soh1p^{MED31} to human MED31p *(19)*.

Class (i) suppressors fell in the essential kinetochore Ndc80 subunit and the kinesin-8 ortholog Klp5, which promotes microtubule catastrophe *(20)*. These mutants might be expected to suppress chromosome mis-segregation defects of RNAi mutants during the two accelerated divisions that *S. pombe* cells undergo at the entry of quiescence (Fig. 1B), as well as in mitosis *(14)* and in meiosis *(21)*. Consistent with this hypothesis, we found that *ndc80*-R523L, *ndc80*-P431L, *ndc80*-R137N and *klp5-del* are TBZ-resistant, similarly to *klp5*Δ *(20)*, and these strains have less rod-shaped cells after 24h in G_0 in a *dcr1*Δ background than the single-mutant *dcr1*Δ (Fig. S6AB). Consistently, the lower suppression by *ndc80*-R137N may indicate that the Ndc80

loop may play a more important role in the suppression, potentially via Dis1 by stabilizing the spindle-microtubule attachment *(18)*. We were additionally able to phenocopy the mis-segregation phenotype in wild-type cells by treatment with TBZ during G_0-entry (24h) (Fig. S6E). Chromosome mis-segregation in RNAi mutants is caused by loss of pericentromeric heterochromatin, and we predicted that restoring pericentromeric heterochromatin in RNAi mutants *(22-24)* should rescue the G_0-entry phenotype. Mutations in the H3K14-acetyltransferase Mst2 complex reduce pericentromeric transcription, allowing heterochromatin to be maintained in a RNAi-independent manner *(22)* and *mst2*Δ indeed strongly rescued the G_0-entry phenotype of RNAi mutants (Fig. S6F).

Class (ii) suppressors suppress the quiescence maintenance defect of *dcr1*Δ (Fig. S5). All suppressors in the CLRC/Rik1 complex lose silencing of the pericentromeric *dg/dh* repeats, and are therefore defective in heterochromatin formation; consistently *raf2*-G37V is mutated in the RFTS (Replication Foci Targeting Sequence) *(25)* while *swi6*-T278K and *swi6*-W293* are mutated in the chromoshadow domain. We subsequently found that *clr4*Δ and *swi6*Δ suppressed *dcr1*Δ, *ago1*Δ and *rdp1*Δ, as did *rik1*Δ (Fig. S7) indicating that H3K9-methylation may be responsible for the progressive loss of viability during G_0 in the absence of RNAi. To investigate this further, we performed ChIP-seq of H3K9me2 in G_0 wild-type and *dcr1*Δ cells (Fig. 3A; Fig. S8; Fig. S9). H3K9me2 localization in wild-type was prevalent at the centromere and subtelomeres, but not at the recently described transient heterochromatic islands found along chromosome arms (Fig. S9), consistent with the observation that these islands disappear following nitrogen-starvation *(26)*. The *dcr1*Δ strain showed near-complete loss of centromeric H3K9me2 (Fig. S8C), as well as at subtelomeric *tlh* loci (Fig. S8B); however, a striking accumulation of H3K9me2 was observed at the rDNA locus (Fig. 3A; Fig. S8A). Intriguingly, H3K9me2 accumulation matched the transcribed region of rDNA (Fig. 3A). H3K9me2 accumulation at the rDNA was also found in wild-type G_0 cells at lower levels and depends on the H3K9 methyltransferase Clr4 (Fig. 3B). This H3K9me2 accumulation continues at longer G_0 times in both wild-type and *dcr1*Δ cells, further increasing the difference between both genotypes as cells enter deeper into quiescence.

To ascertain that the suppression effect of CLRC/Rik1 mutants is mediated by loss of H3K9me2 and not through a potential new target of the complex, we created a set of prototroph strains to assay histone H3 mutants in G_0 (*hht3*Δ *hht1*-K9R *hht2*-K9R), keeping viability for over a week *(15)* (Fig. S10A). The *dcr1*Δ*hht3*Δ *hht1*-K9R *hht2*-K9R strains rescued G_0 viability (Fig. S10B); and interestingly, the reduction of H3K9me2 in *dcr1*Δ*hht3*Δ *hht1*-K9R and in *dcr1*Δ*hht3*Δ *hht2*-K9R strains alone was also sufficient to recover G_0 viability (Fig. S10BC). These results confirm that H3K9me2 is central to the quiescence maintenance defect of *dcr1*Δ cells. We then attempted to increase the levels of H3K9me at the rDNA to see if the defect would be enhanced. As the recruitment factor for Clr4 at rDNA in G_0 is unknown, we decided instead to increase global Clr4 levels in G_0. We replaced the promoter of *clr4* at its endogenous location by the promoter of *urg1* (Fig. S11A), which is induced not only by uracil but also by nitrogen-starvation *(15, 27)*. The resulting *purg1-clr4* strain entered G_0 with wild-type viability but over-accumulated H3K9me2 at rDNA and quickly lost viability specifically in quiescence maintenance (Fig. S11BC); in the *dcr1*Δ *purg1-clr4* background, the H3K9me2 rDNA accumulation was increased even further, resulting in very low viability, almost complete after a week in G_0 (Fig. S11BC). However as the accumulation of H3K9me2 is not specific to the rDNA in these strains, we cannot exclude that other genomic locations participate in the loss of viability in this assay, via silencing of essential genes.

The class (iii) suppressors also suppressed the quiescence maintenance defect (Fig. S5). These suppressor mutations lay in RNA polymerase factors: $Tbp1^{TBP}$ (in RNA pol I, II and III) *(28)* and the Mediator complex, a co-regulator of RNA pol II, which may also play a role in transcription by other RNA polymerases *(29)*. These genes act upstream of rDNA heterochromatinization, as H3K9me2 at rDNA is reduced in *dcr1*Δ *med31-ins* and *dcr1*Δ *tbp1*-D156Y G_0 cells (Fig. 4H). Interestingly, the strong suppressor *med31-ins* also suppresses G_0-entry and TBZ-sensitivity (Fig. S5), and might therefore additionally act at centromeric heterochromatin, similarly to *mst2*Δ and the Mediator subunit *pmc2*Δ *(22)*. In support of this idea, distinct subunits of Mediator have been shown to play a role in silencing *(30)* and anti-silencing *(22)*. In dividing cells, Dicer is required for efficient RNA polymerase II termination at various genomic locations including centromeres, tDNAs, and rDNA, and stalled RNA pol II accumulates in *dcr1*Δ at these loci *(31)* (Fig. S12). We performed ChIP-seq using an antibody directed against RNA pol II (unphosphorylated CTD)

in wild-type and *dcr1*Δ G_0 cells, but in contrast to the situation in cycling cells *(31)*, no significant increase was detected at the rDNA in *dcr1*Δ G_0 cells (Fig. S12). ChIP-qPCR using antibodies against the phosphorylated CTD pol II (S2P, S5P) did not show significant differences either. Small RNA sequencing revealed that, in G_0 cells, centromeric small RNAs were strongly reduced at pericentromeric regions (Fig. S14AB), as well as other siRNAs, consistent with their production in the G_1- and S-phases of the cell cycle *(32)*. Furthermore, in contrast to the situation in cycling cells *(31)*, no small RNA antisense to the rRNA were found (Fig. S14C), and we did not detect any new loci of Dicer-dependent small RNA production in G_0 cells *(15)*.

We therefore decided to assay RNA polymerase I, which is responsible for rDNA transcription. RNA pol I occupancy at rDNA, assayed by ChIP-qPCR of tagged $Nuc1^{RPA190}$ *(15)* (Fig. 4A), was lower than wild type in cycling *dcr1*Δ cells, likely due to the slightly reduced growth rate of *dcr1*Δ due to accumulation of DNA damage *(10, 31)* (Fig. 4C; Fig. S15B). There was no significant difference in RNA pol I occupancy between wild-type and *dcr1*Δ initially in G_0, but strikingly we saw that RNA pol I occupancy is further reduced as cells enter into deeper quiescence, and that *dcr1*Δ cells do not have this reduction, indicative of a failure to release RNA pol I (Fig. 4DEF). This accumulation is detected at the 5'ETS, 18S, 5.8S, 28S repeats, as well as at the very end of the 3'ETS next to the termination site Ter3. Strikingly, the accumulation of RNA pol I was not reduced in *dcr1*Δ*clr4*Δ, suggesting that failure to release RNA pol I lies upstream of H3K9me accumulation. In contrast, RNA pol I occupancy was strongly reduced in *dcr1*Δ*tbp1*-D156Y, and slightly reduced in *dcr1*Δ*med31-ins*, providing an explanation for their suppression effect, as well as for their reduced accumulation of H3K9me2 (Fig. 4GH).

The failure to release RNA pol I at rDNA in G_0 may result in DNA damage, similar to the failure to release RNA pol II at centromeres and rDNA in the cell cycle *(31)*. As G_0 cells do not rely on HR for DNA repair, *rad22*-YFP foci are not formed in quiescent 1c cells *(8)*, although we observed that they strongly accumulate upon G_0-exit of *dcr1*Δ (Fig. S13BF). We therefore used H2A and H2A-S129phos (equivalent to γH2AX) antibodies to assay DNA damage directly in G_0 cells by both ChIP-seq and ChIP-qPCR in wt and *dcr1*Δ, and observed an increase in rDNA in *dcr1*Δ cells (Fig. S13AC). The H2A-S129phos/H2A ratio was reduced in suppressors rescuing the RNA pol I defect, *dcr1*Δ*tbp1*-D156Y and *dcr1*Δ*med31-ins* (Fig. S13C); the absence of

reduction in *dcr1*Δ*clr4*Δ suggests that DNA damage accumulation is correlated to stalled RNA pol I at the rDNA, but that the primary cause of death is not DNA damage itself but rather the accumulation of H3K9me2.

We further explored the distinction between RNA pol II release during S-phase and RNA pol I release during G_0 by constructing a *dcr1*Δ*reb1*Δ double mutant strain: $Reb1^{TTFI}$ is a factor that participates in RNA pol I termination and forces the direction of replication to occur in the same direction as transcription at the rDNA, thus avoiding collisions between DNA and RNA polymerase *(33)*. While *reb1*Δ cells are viable, the accumulation of RNA pol II in *dcr1*Δ may increase the need for Reb1 in order to avoid polymerase collisions and subsequent DNA damage at the rDNA. In accordance with this hypothesis, *dcr1*Δ*reb1*Δ strains show a strong negative epistatic interaction in dividing cells resulting in extremely poor growth (Fig. S15B); however, their viability is unaffected in G_0, and is similar to the *dcr1*Δ single-mutant (Fig. S15A).

If RNA polymerase I is responsible for the quiescence maintenance defect of *dcr1*Δ, we reasoned that deletion of non-essential subunits of RNA pol I may destabilize it, and therefore, similarly to class (iii) suppressors, would allow RNAi-independent release. We therefore assayed *rpa12*Δ mutants in G_0. Rpa12 is a non-essential subunit of RNA pol I required for polymerase termination *(34)*, and strikingly, we found that *dcr1*Δ*rpa12*Δ suppressed the quiescence maintenance defect (Fig. S15C), although it does not affect H3K9me2 levels at the rDNA. We were unfortunately unable to assay RNA pol I levels in these cells as *nuc1*-FLAG *rpa12*Δ double-mutants are inviable, most likely because RNA pol I becomes too unstable in this background. Thus, Rpa12 can be considered a "class iv" suppressor. As the suppressor screen is not saturated yet, we predict that sequencing many more of the >50 suppressors we obtained will yield interesting alleles in RNA polymerase-associated factors in both class iii (general transcription) and iv (RNA pol I). We propose in particular that the specific recruitment factor responsible for rDNA H3K9me2 increase in G_0 could be a subunit of RNA pol I itself, providing a potential explanation as to why it would be difficult to recover such a suppressor.

We have identified RNAi as a novel essential regulator of quiescence in *S. pombe.* RNAi both promotes heterochromatin formation at centromeres allowing proper chromosome segregation

during G_0-entry, and prevents heterochromatin formation at the rDNA locus during quiescence maintenance (Fig. S16). At G_0-entry, mis-segregation results in cell death, and can be suppressed by restoring heterochromatin or by strengthening segregation. In dividing cells RNAi is required to release RNA pol II from rDNA and from pericentromeric heterochromatin, and in RNAi mutants pol II must be removed from stalled replication forks by homologous recombination repair (HR) *(10)*, resulting in a severe reduction in rDNA copy number *(31)*. G_0 cells possess a 1c DNA content and therefore use non-homologous end-joining (NHEJ) instead of HR for repair *(8)*. Consistently, rDNA copies are not lost in RNAi mutants during quiescence. During quiescence maintenance, RNAi is required to release RNA pol I from rDNA. The failure to release RNA pol I results in over-recruitment of rDNA silencing factors, possibly by RNA pol I itself; in mammalian cells *(35)*, rRNA interacts with SUV39H1 via NML *(36)* and RNA pol I interacts with the G9a methyltransferase *(37)*. Stalled RNA pol I results in an over-accumulation of H3K9me2 at rDNA, and DNA damage, resulting in loss of viability of these cells, similarly to when essential genes are silenced by H3K9me2 *(38)*. These defects can be suppressed by mutants in the silencing CLRC/Rik1 complex, the effector $Swi6^{HP1}$, and specific mutants in RNA pol I non-essential subunits. Both RNA pol II and RNA pol I defects can be suppressed by specific alleles in the key transcription TATA Binding Protein (TBP) and Mediator (Med) complexes.

Thus each class of suppressors illuminates key roles of RNAi in quiescent cells: in chromosome segregation, in heterochromatin formation and spreading, and in transcription. As spontaneous mutations in essential genes are much more rare, we obtained relatively few class (iii) suppressors, and none from class (iv). We expect that saturation of the G_0 screen may uncover the precise components of RNA polymerase I, or rDNA-associated factors, involved in recruiting the CLRC/Rik1 complex for G_0 rDNA silencing, and more 'master regulators' genes which, like Dicer and TBP, regulate transcription by all RNA polymerases.

The rDNA locus plays a central role in ageing *(39)* and H3K9me is a hallmark of rDNA silencing in plants *(40)* as well as in mammalian cells *(36)*. The role of RNAi at rDNA may also be evolutionarily conserved; in mammalian cells Dicer physically associates with rDNA *(41)*, while in *Candida albicans* Dicer is involved in pre-rRNA processing by cleaving the 3'ETS *(42)*. In *Neurospora crassa* quelling (RNAi) targets rDNA *(43)*, and qiRNAs are generated at the rDNA

locus by Dicer when cells are treated with alkylating agents or with hydroxyurea *(44)*. Furthermore, there is evidence that during evolution RNAi and heterochromatin proteins (H3K9me, HP1) have been lost together, a loss which has happened independently in distinct fungal lineages such as budding yeasts of the subphylum Saccharomycotina *(45)*, *Ustilago maydis* (Basidiomycota, subphylum Ustilagomycotina) *(46)*, and the human pathogen *Pneumocystis jirovecii* (Ascomycota, subphylum Taphrinomycotina) *(47)*. In budding yeasts, the loss of RNAi is correlated with the ability to acquire Killer RNA viruses *(48)*. Our results provide a possible explanation for a strong selective pressure to lose H3K9me-based heterochromatin upon RNAi loss, accounting for their co-dependency in eukaryotic evolution.

Our finding sheds light on the anecdotal observation that some mutants in *S. pombe*, like *dcr1*Δ, do not keep well in long-term storage at low temperatures. We have found that repeated thawing/freezing cycles can select for spontaneous suppressors, which are quite widespread in laboratory strains of RNAi mutants. RNAi mutants also fail to differentiate into dormancy in asexual and sexual spores in *Cryptococcus neoformans,* an important human basidiomycete pathogen *(49)*, and in the zygomycete *Mucor circinelloides (50)*. In metazoans, such as *Cænorhabditis elegans (51)* and *Drosophila melanogaster (52)*, Dicer mutants typically affect germ cells, which also spend long periods in quiescence. Given the importance of quiescence in the life cycle of unicellular as well as multicellular organisms, it is likely that epigenetic pathways will be found to be essential in neurons, germ cells and cancer stem cells, which can spend many years in a quiescent state. Uncovering the mechanisms underlying the epigenetic regulation of quiescence thus opens a promising new field of study.

References and Notes:

1. T. H. Cheung, T. A. Rando, Molecular regulation of stem cell quiescence. *Nat. Rev. Mol. Cell. Biol.* **14**, 329-340 (2013).

2. P. Codega *et al.* Prospective identification and purification of quiescent adult neural stem cells from their in vivo niche. *Neuron* **82**, 545-559 (2014).

3. A. Okhrimenko *et al.* Human memory T cells from the bone marrow are resting and maintain long-lasting systemic memory. *Proc. Nat. Acad. Sci. U.S.A.* **111**, 9229-9234 (2014).

4. S. S. Su, Y. Tanaka, I. Samejima, K. Tanaka, M. Yanagida. A nitrogen starvation-induced dormant G_0 state in fission yeast: the establishment from uncommitted G_1 state and its delay for return to proliferation. *J. Cell. Sci.* **109**, 1347-1357 (1996).

5. E. S. Ritterhaus, S. H. Baek, C. M. Sassetti. The normalcy of dormancy: common themes in microbial quiescence. *Cell Host Microbe* **13**, 643-651 (2013).

6. M. Shimanuki *et al.* Two-step, extensive alterations in the transcriptome from G_0 arrest to cell division in *Schizosaccharomyces pombe*. *Genes Cells* **12**, 677-692 (2007).

7. S. Marguerat *et al.* Quantitative analysis of fission yeast transcriptomes and proteomes in proliferating and quiescent cells. *Cell* **151**, 671-683 (2012).

8. S. Mochida, M. Yanagida. Distinct modes of DNA damage response in *S. pombe* G_0 and vegetative cells. *Genes Cells* **11**, 13-27 (2006).

9. K. Takeda *et al.* Synergistic roles of the proteasome and autophagy for mitochondrial maintenance and chronological lifespan in fission yeast. *Proc. Nat. Acad. Sci. U.S.A.* **107**, 3540-3545 (2010).

10 M. Zaratiegui *et al.* RNAi promotes heterochromatic silencing through replication-coupled release of RNA pol II. *Nature* **479**, 135-138 (2011).

11. S. E. Castel, R. A. Martienssen. RNA interference in the nucleus: roles for small RNAs in transcription, epigenetics and beyond. *Nat. Rev. Genet.* **14**, 100-112 (2013).

12. F. Li, R. A. Martienssen, W. Z. Cande. Coordination of DNA replication and histone modification by the Rik1-Dos2 complex. *Nature* **475**, 244-248 (2011).

13. T. A. Volpe *et al.* Regulation of heterochromatic silencing and histone H3 lysine-9 methylation by RNAi. *Science* **297**, 1833-1837 (2002).

14. T. A. Volpe *et al.* RNA interference is required for normal centromere function in fission yeast. *Chromosome Res.* **11**, 137-146 (2003).

15. Materials and methods are available as supplementary materials on *Science* Online.

16. S. Ben Hassine, B. Arcangioli. Tdp1 protects against oxidative DNA damage in non-dividing fission yeast. *EMBO J.* **28**, 632-640 (2009).

17. D. V. Irvine *et al.* Mapping epigenetic mutations in fission yeast using whole-genome next-generation sequencing. *Genome Res.* **19**, 1077-1083 (2009).

18. K. S. Tsu, T. Toda. Ndc80 internal loop interacts with Dis1/TOG to ensure proper kinetochore-spindle attachment in fission yeast. *Curr. Biol.* **21**, 214-220 (2011).

19. T. Linder, C. M. Gustafsson. The Soh1/MED31 protein is an ancient component of Schizosaccharomyces pombe and Saccharomyces cerevisiae Mediator. *J. Biol. Chem.* **279**, 49455-49459 (2004).

20. R. R. West, T. Malmstrom, C. L. Troxell, J. R. McIntosh. Two related kinesins, *klp5+* and *klp6+*, foster microtubule disassembly and are required for meiosis in fission yeast. *Mol. Biol. Cell* **12**, 3919-3932 (2001).

21. I. M. Hall, K. Noma, S. I. Grewal. RNA interference machinery regulates chromosome dynamics during mitosis and meiosis in fission yeast. *Proc. Nat. Acad. Sci. U.S.A.* **100**, 193-198 (2003).

22. B. D. Reddy *et al.* Elimination of a specific histone H3K14 acetyltransferase complex bypasses the RNAi pathway to regulate pericentric heterochromatin functions. *Genes Dev.* **25**, 214-219 (2011).

23. F. E. Reyes-Turcu, K. Zhang, M. Zofall, E. Chen, S. I. Grewal. Defects in RNA quality control factors reveal RNAi-independent nucleation of heterochromatin. *Nat. Struct. Mol. Biol.* **18**, 1132-1138 (2011).

24. Tadeo *et al.* Elimination of shelterin components bypasses RNAi for pericentric heterochromatin assembly. *Genes Dev.* **27**, 2489-2499 (2013).

25. S. A. White *et al.* The RFTS domain of Raf2 is required for Cul4 interaction and heterochromatin integrity in fission yeast. *PLoS One* **9**:e104161 (2014), doi:10.1371/journal.pone.0104161.

26. M. Zofall *et al.* RNA elimination machinery targeting meiotic mRNAs promotes facultative heterochromatin formation. *Science* **335**, 96-100 (2012).

27. S. Watt *et al.* urg1: a uracil-regulatable promoter system for fission yeast with short induction and repression times. *PLoS One* **3**:e1428 (2008), doi:10.1371/journal.pone.0001428.

28. M. Hamada, Y. Huang, T. M. Lowe, R. J. Maraia. Widespread use of TATA elements in the core promoters for RNA polymerases III, II, and I in fission yeast. *Mol. Cell. Biol.* **21**, 6870-6881 (2001).

29. J. O. Carlsten, X. Zhu, M. D. López, T. Samuelsson, C. M. Gustafsson. Loss of the Mediator subunit Med20 affects transcription of tRNA and other non-coding RNA genes in fission yeast. *Biochim. Biophys. Acta* **1859**, 339-347 (2016).

30. M. Thorsen, H. Hansen, M. Venturi, S. Homlberg, G. Thon. Mediator regulates non-coding RNA transcription at fission yeast centromeres. *Epigenetics Chromatin* **5**:19 (2012), doi:10.1186/1756-8935-5-19.

31. S. E. Castel *et al.* Dicer promotes transcription termination at sites of replication stress to maintain genome stability. *Cell* **159**, 572-583 (2014).

32. A. Kloc, M. Zaratiegui, E. Nora, R.A. Martienssen. RNA interference guides histone modification during the S phase of chromosomal replication. *Curr. Biol.* **18**, 490-495 (2008).

33. A. Sánchez-Gorostiaga, C. López-Estraño, D. B. Krimer, J. B. Schvartzman, P. Hernández. Transcription termination factor reb1p causes two replication fork barriers at its cognate sites in fission yeast ribosomal DNA in vivo. *Mol. Cell. Biol.* **24**, 398-406.

34. E. M. Prescott *et al.* Transcriptional termination by RNA polymerase I requires the small subunit Rpa12p. *Proc. Nat. Acad. Sci. U.S.A.* **101(16)**, 6068-6073 (2004).

35. R. Voit and I. Grummt. The RNA polymerase I transcription machinery. In: The Nucleolus, M. Olson, Ed., vol. 15 of *Springer Protein Reviews* (2011).

36. A. Murayama *et al.* Epigenetic control of rDNA loci in response to intracellular energy status. *Cell* **133**, 627-639 (2008), doi:10.1016/j.cell.2008.03.030.

37. X. Yuan, W. Feng, A. Imhof, I. Grummt, Y. Zhou. Activation of RNA polymerase I transcription by cockayne syndrome group B protein and histone methyltransferase G9a. *Mol. Cell.* **27**, 585-595 (2007).

38. J. Wang, B. D. Reddy, S. Jia. Rapid epigenetic adaptation to uncontrolled heterochromatin spreading. *Elife* **4** (2015), doi:10.7554/eLife.06179.

39. A. R. Ganley, T. Kobayashi. Ribosomal DNA and cellular senescence: new evidence supporting the connection between rDNA and aging. *FEMS Yeast Res.* **14**, 49-59 (2014), doi:10.1111/1567-1364.12133.

40. F. Pontvianne *et al.* Histone methyltransferases regulating rRNA gene dose and dosage control in Arabidopsis. *Genes Dev.* **26**, 945-957 (2012), doi:10.1101/gad.182865.111.

41. L. Sinkkonen, T. Hugenschmidt, W. Filipowicz, P. Svoboda. Dicer is associated with ribosomal DNA chromatin in mammalian cells. *PLoS One* **5**:e12175 (2010), doi:10.1371/journal.pone.0012175.

42. D. A. Bernstein *et al.* Candida albicans Dicer (CaDcr1) is required for efficient ribosomal and spliceosomal RNA maturation. *Proc. Nat. Acad. Sci. U.S.A.* **109**, 523-528 (2012).

43. G. Cecere, C. Cogoni. Quelling targets the rDNA locus and functions in rDNA copy number control. *BMC Microbiol.* **9**:44 (2009), doi:10.1186/1471-2180-9-44.

44. Z. Zhang *et al.* Homologous recombination as a mechanism to recognize repetitive DNA sequences in an RNAi pathway. *Genes Dev.* **27**:145-150 (2013), doi:10.1101/gad.209494.112.

45. I. A. Drinnenberg *et al.* RNAi in budding yeast. *Science* **326**, 544-550 (2009).

46. J. D. Laurie *et al.* Genome comparison of barley and maize smut fungi reveals targeted loss of RNA silencing components and species-specific presence of transposable elements. *Plant Cell* **24**, 1733-1745 (2012).

47. O. H. Cissé, M. Pagni, P. M. Hauser. Comparative genomics suggests that the human pathogenic fungus *Pneumocystis jirovecii* acquired obligate biotrophy through gene loss. *Genome Biol. Evol.* **6**, 1938-1948 (2014).

48. I. A. Drinnenberg, G. R. Fink, D. P. Bartel. Compatibility with killer explains the rise of RNAi-deficient fungi. *Science* **333**, 1592 (2011), doi:10.1126/science.1209575.

49. X. Wang *et al.* Sex-induced silencing defends the genome of *Cryptococcus neoformans* via RNAi. *Genes Dev.* **24**, 2566-2582 (2010), doi:10.1101/gad.1970910.

50. J. P. de Haro *et al.* A single dicer gene is required for efficient gene silencing associated with two classes of small antisense RNAs in *Mucor circinelloides*. *Eukaryot. Cell* **8**, 1486-1497 (2009), doi:10.1128/EC.00191-09.

51. R. F. Ketting *et al.* Dicer functions in RNA interference and in synthesis of small RNA involved in developmental timing in *C. elegans*. *Genes Dev.* **15**, 2654-2659 (2001).

52. Z. Jin, T. Xie. Dcr-1 maintains Drosophila ovarian stem cells. *Curr. Biol.* **17**, 539-544 (2007).

53. B. Langmead, S. L. Salzberg. Fast gapped-read alignment with Bowtie 2. *Nat. Methods* **9**, 357-359 (2012), doi:10.1038/nmeth.1923.

54. H. Li *et al.* The Sequence Alignment/Map format and SAMtools. *Bioinformatics* **25**, 2078-2079 (2009), doi:10.1093/bioinformatics/btp352.

55. E. Garrison, G. Marth. Haplotype-based variant detection from short-read sequencing. arXiv:1207.3907v2 (2012).

56. A. R. Quinlan, I. M. Hall. BEDTools: a flexible suite of utilities for comparing genomic features. *Bioinformatics* **26**, 841-842 (2010), doi:10.1093/bioinformatics/btq033.

57. P. Danecek *et al.* The variant call format and VCFtools. *Bioinformatics* **27**, 2156-2158 (2011), doi:10.1093/bioinformatics/btr330.

58. M. Martin. Cutadapt removes adapter sequences from high-throughput sequencing reads. *EMBnet.journal* (2011), doi:10.14806/ej.17.1.200.

59. B. Langmead, C. Trapnell, M. Pop, S. L. Salzberg. Ultrafast and memory-efficient alignment of short DNA sequences to the human genome. *Genome Biol.* **10**, doi:10.1186/gb-2009-10-3-r25 (2009).

Supplementary Materials

www.sciencemag.org

Materials and Methods

Figs. S1 to S16

Tables S1 to S3

Acknowledgments:

This work was funded by NIH grant R01 GM076396-08 and by the Howard Hughes Medical Institute and Gordon & Betty Moore Foundation Plant Biology Investigator Program [to R.M.]. The authors acknowledge support from the Chaire Blaise Pascal (Fondation de l'École Normale Supérieure, France). We would like to thank the Cold Spring Harbor Laboratory Woodbury Sequencing Facility. We would like to thank everyone at the fission yeast database PomBase, as its resources have been extremely helpful for research in our lab. We would also like to thank the reviewers for their helpful comments and suggestions. The raw data of the next-generation sequencing libraries reported in this paper are available at the Sequence Read Archive (SRA) database, accession number SRP087488 (BioProject PRJNA341984). The authors report no conflicts of interest.

Figure legends:

Figure 1. RNAi mutants lose viability in G_0.

(A) Loss of viability at both G_0-entry and during quiescence maintenance in prototroph *dcr1*Δ, *rdp1*Δ and *ago1*Δ mutants (n=5 biological replicates for wild-type, n=6 for *dcr1*Δ and *rdp1*Δ, n=7 for *ago1*Δ). ** indicates a statistically significant difference ($p<0.01$, t-test) between each mutant and wt for all time-points, and between time-points 24h and 15 days (B) Microscopic observation of DAPI-stained RNAi mutants reveals an increased proportion of cells retaining a rod-shape in early G_0 (24h). After 15 days, while wild-type G_0 cells look uniform, RNAi mutants display a variety of morphological defects and many dead refraction-negative and/or DAPI-negative cells. Upon G_0-entry (C) RNAi mutants have a reduction in the increase in cell number found in wild type cells during the initial two divisions (24h G_0; n=2; ** $p<0.01$), and (D) an increase in the number of cells staying rod-shaped (24h G_0; n=2; * $p<0.05$, ** $p<0.01$). All error bars indicate standard deviation; n indicates biological replicates.

Figure 2. Design of a G_0 suppressor screen.

(A) Experimental design of the suppressor screen: a *dcr1*Δ population is alternated between the cell cycle (in rich medium, YES) and quiescence (in nitrogen-deprived medium, EMM-N) every 1 to 3 days. Spontaneous suppressors, by their relative fitness advantage compared to the parental strain, get enriched during the alternations. After up to 20 alternations, individual clones are isolated and re-assayed in G_0 to check for suppression. (B) Summary of mutations present in 13

isolated *dcr1*Δ G_0 suppressors showing three classes of mutants, in chromosome segregation, the CLRC/Rik1 complex and $Swi6^{HP1}$, and RNA polymerase-associated factors. Each mutation in the list arose as an independent suppressor.

Figure 3. Quiescence maintenance of *dcr1*Δ results in rDNA heterochromatinization by H3K9me.

(A) H3K9me2 ChIP-seq enrichment in *dcr1*Δ vs. *wt* cells. In G_0 cells, but not cycling cells, *dcr1*Δ strongly accumulates H3K9me2 at the rDNA locus (n=2 biological replicates, cycling cell data from *(31)*). (B) Validation by H3K9me2 ChIP-qPCR in wild-type and *dcr1*Δ cycling and G_0 cells shows a stronger rDNA H3K9me2 increase in G_0 cells in *dcr1*Δ as compared to wild-type G_0 cells (n≥3 biological replicates; ** $p<0.01$, t-test).

Figure 4. *dcr1*Δ mutants are defective in RNA polymerase I release in quiescence maintenance.

(A) The main subunit of RNA polymerase I $Nuc1^{RPA190}$ was tagged with a $(Gly)_6$ linker and 3xFLAG. (B) Probe location for ChIP-qPCRs: 1: rDNA promoter, 2: 5'ETS, 3: 18S, 4: 3'ETS. (C) RNA polymerase I enrichment at the rDNA was assayed by ChIP-qPCR using anti-FLAG antibody in the *nuc1*-$(Gly)_6$-FLAG background, showing an higher occupancy in wild-type than *dcr1*Δ mutants in cycling cells, due to the reduced growth rate of *dcr1*Δ, and (D) a similar occupancy in early G_0 cells (n=2 biological replicates). (E, F) RNA polymerase I enrichment at 18S rDNA over time spent in G_0 (2 to 8 days) shows a reduction in wild-type cells, but *dcr1*Δ cells fail to release RNA pol I (n≥2 biological replicates). (G) The class (iii) suppressors, *dcr1*Δ *tbp1*-D156Y and *dcr1*Δ*med31-ins*, but not the class (ii) suppressor *dcr1*Δ*clr4*Δ, significantly decrease RNA polymerase I occupancy at rDNA in 8 days G_0 cells. (n=2 biological replicates, * $p<0.05$, ** $p<0.01$, t-test) (H) The accumulation of H3K9me2 at rDNA repeats, assayed by ChIP-qPCR, is significantly reduced in class (iii) suppressors (n≥3 biological replicates, ** $p<0.01$, t-test).

Figure 1:

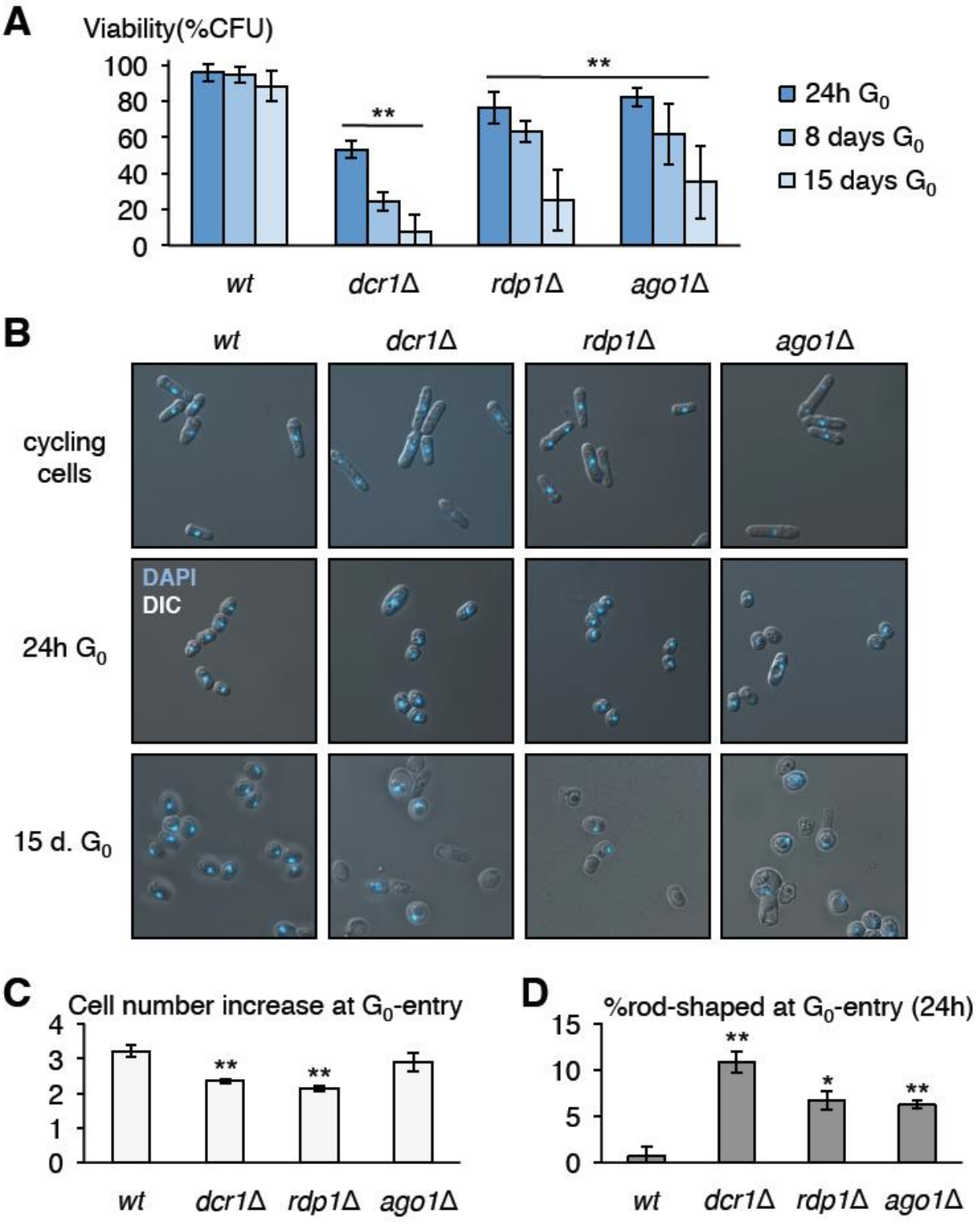
A
Viability(%CFU)
100
80
60
40
20
0
**
**
24h G0
8 days G0
15 days G0
wt
dcr1Δ
rdp1Δ
ago1Δ
B
wt
dcr1Δ
rdp1Δ
ago1Δ
cycling cells
24h G0
15 d. G0
DAPI
DIC
C
Cell number increase at G0-entry
4
3
2
1
0
**
**
wt
dcr1Δ
rdp1Δ
ago1Δ
D
%rod-shaped at G0-entry (24h)
15
10
5
0
**
*
**
wt
dcr1Δ
rdp1Δ
ago1Δ

Figure 2:

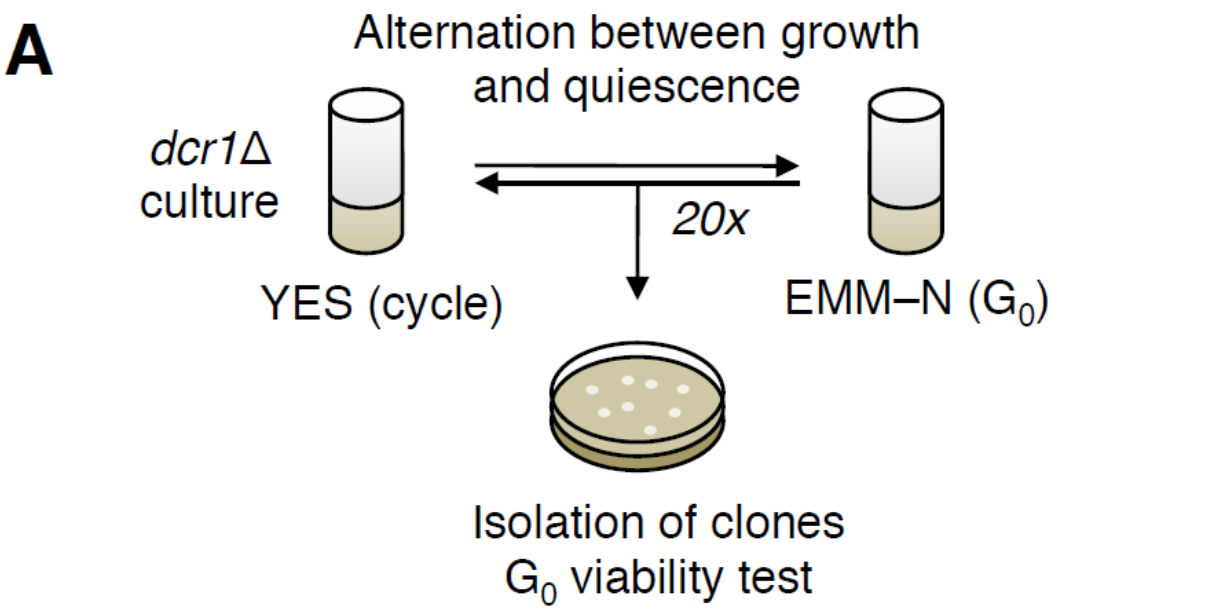

B

Chromosome segregation	CLRC/Rik1 silencing complex	RNA polymerase associated factors
ndc80-R523L	*rik1*-K812*	*tbp1*-D156Y
ndc80-P431L	*rik1*-T942K	*med31-ins*
ndc80-R137N	*raf2*-G37V	
klp5-del	*clr4*-R126*	
	clr4-Y451*	
	swi6-T278K	
	swi6-W293*	

Figure 3:

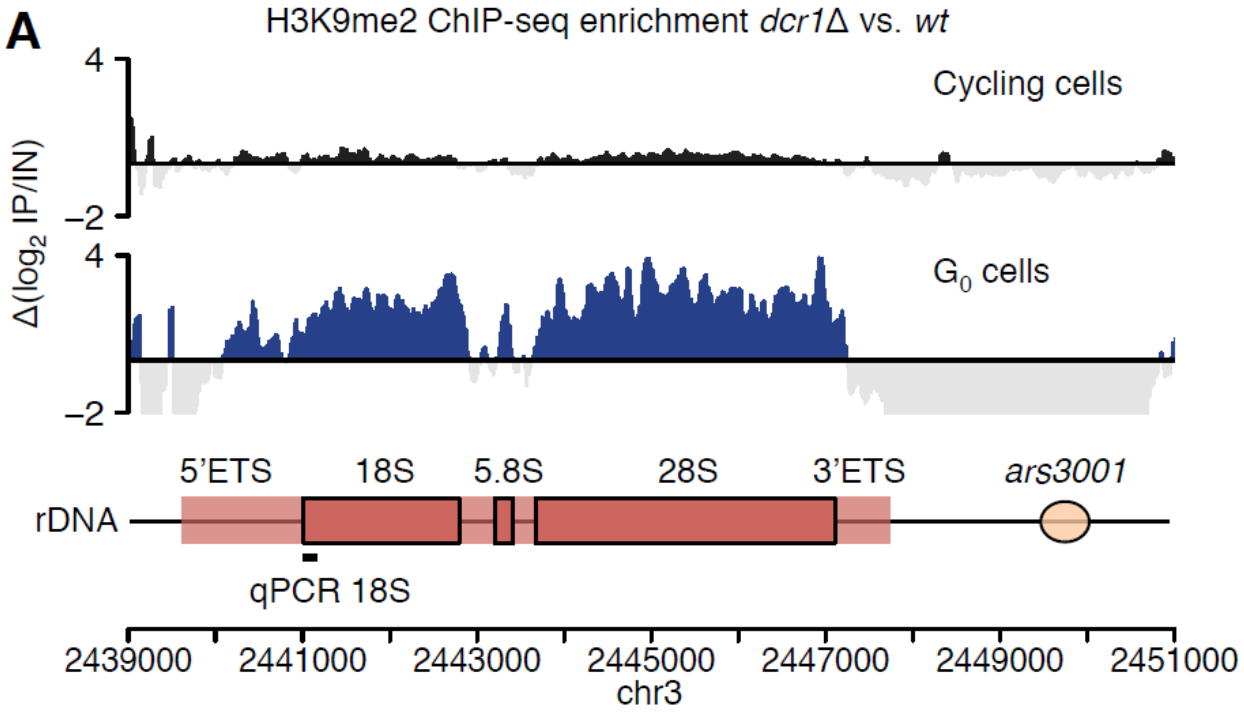
A
H3K9me2 ChIP-seq enrichment dcr1Δ vs. wt
Cycling cells
G0 cells
Δ(log2 IP/IN)
4
−2
5'ETS
18S
5.8S
28S
3'ETS
ars3001
rDNA
qPCR 18S
2439000
2441000
2443000
2445000
2447000
2449000
2451000
chr3

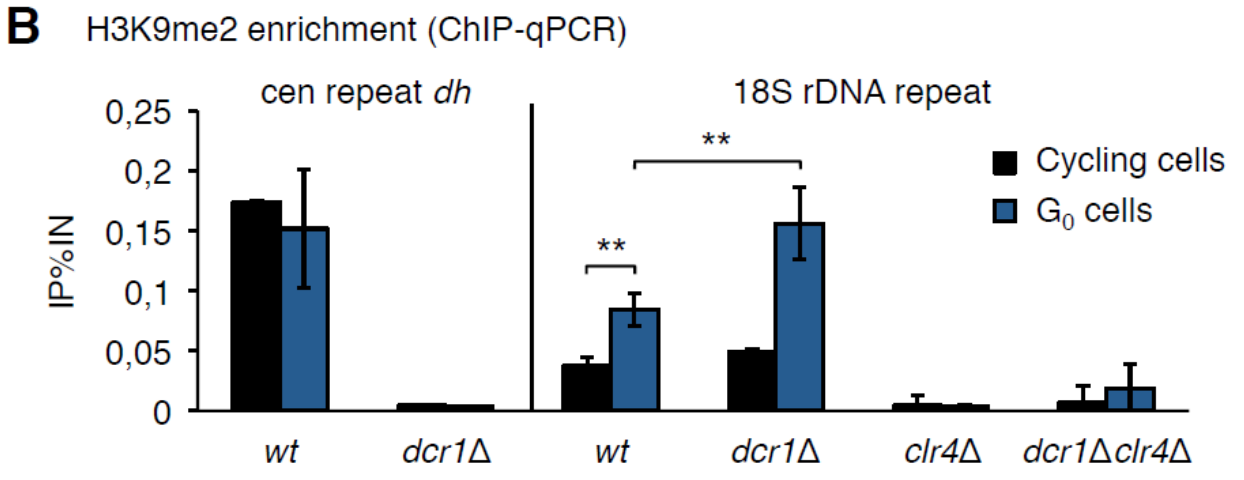
B
H3K9me2 enrichment (ChIP-qPCR)
cen repeat dh
18S rDNA repeat
IP%IN
0,25
0,2
0,15
0,1
0,05
0
**
**
Cycling cells
G0 cells
wt
dcr1Δ
wt
dcr1Δ
clr4Δ
dcr1Δclr4Δ

Figure 4:

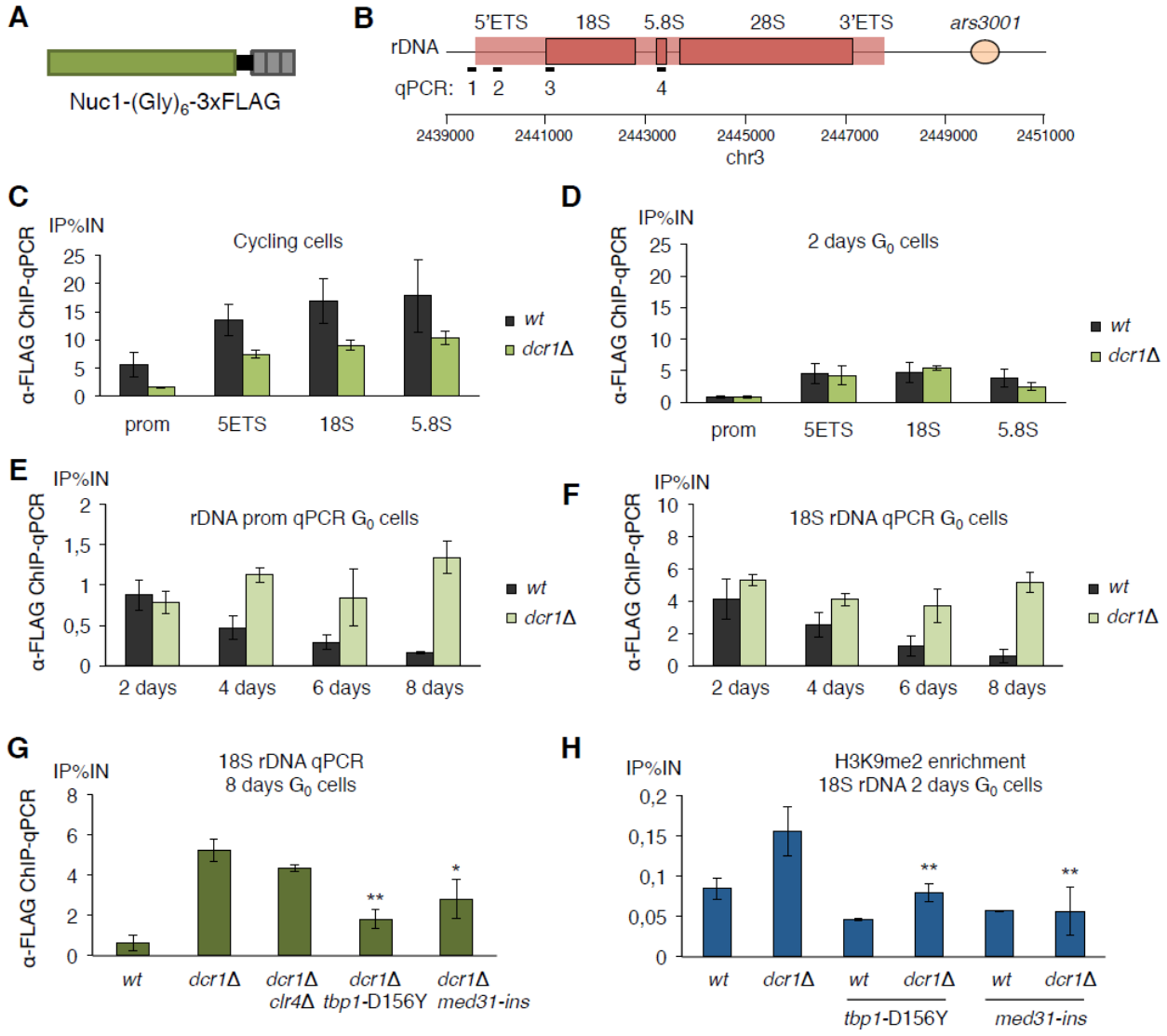
A
Nuc1-(Gly)6-3xFLAG
B
5'ETS
18S
5.8S
28S
3'ETS
ars3001
rDNA
qPCR: 1 2 3 4
2439000
2441000
2443000
2445000
2447000
2449000
2451000
chr3
C
IP%IN
α-FLAG ChIP-qPCR
Cycling cells
wt
dcr1Δ
prom
5ETS
18S
5.8S
D
2 days G0 cells
E
rDNA prom qPCR G0 cells
2 days
4 days
6 days
8 days
F
18S rDNA qPCR G0 cells
G
18S rDNA qPCR
8 days G0 cells
dcr1Δ clr4Δ
dcr1Δ tbp1-D156Y
dcr1Δ med31-ins
H
H3K9me2 enrichment
18S rDNA 2 days G0 cells
tbp1-D156Y
med31-ins